Acta Crystallographica Section F
Structural Biology and Crystallization Communications
ISSN 1744-3091

On-column ligand exchange for structure-based drug design: a case study with human 11β-hydroxysteroid dehydrogenase type 1

Wenying Qin,[a] Russell A. Judge,[b]* Kenton L. Longenecker,[b] Larry R. Solomon[b] and John E. Harlan[b]

[a]Consultant, 11 Minute Man Lane, Lexington, MA 02421, USA, and [b]Global Pharmaceutical Research and Development, Abbott Laboratories, 100 Abbott Park Road, Abbott Park, IL 60064, USA

Correspondence e-mail: russell.judge@abbott.com

Received 30 November 2011
Accepted 7 March 2012

Successfully forming ligand–protein complexes with specific compounds can be a significant challenge in supporting structure-based drug design for a given protein target. In this respect, an on-column ligand- and detergent-exchange method was developed to obtain ligand–protein complexes of an adamantane series of compounds with 11β-hydroxysteroid dehydrogenase type 1 (11β-HSD1) after a variety of other complexation methods had failed. This report describes the on-column exchange method and an unexpected byproduct of the method in which artificial trimers were observed in the structures.

1. Introduction

One of the challenges in structure-based drug design is obtaining structures of the target protein with specific chemical compounds. Often, these compounds are identified from compound screens or are synthesized as part of lead-optimization activities. Depending on the chemical matter, it can be problematic to make the ligand–protein complexes required for crystallization and structure determination. In these attempts a number of complexation methods are commonly used, including soaking, displacement soaking, cocrystallization with ligands, adding ligands during purification, solution ligand exchange prior to crystallization or co-expression of the target protein with ligands (Hassell *et al.*, 2007). In a structure-based drug-design effort with 11β-hydroxysteroid dehydrogenase type 1 (11β-HSD1), obtaining structures with specific adamantane-based ligands proved to be particularly problematic.

11β-HSD1, an NADPH-dependent enzyme, is the principal enzyme in humans that catalyzes the conversion of the inactive glucocorticoid cortisone to the active glucocorticoid cortisol (Tomlinson *et al.*, 2004). The isoform 11β-HSD2 catalyses the reverse reaction and together they regulate tissue-specific glucocorticoid levels (Asensio *et al.*, 2004; Tomlinson *et al.*, 2004). Glucocorticoids are steroid hormones that are important regulators of glucose production and lipid homeostasis in tissues. Glucocorticoid excess in tissues can lead to obesity or metabolic syndrome, expressed as central obesity, insulin resistance or glucose intolerance, dyslipidemia and hypertension (Asensio *et al.*, 2004; Rosmond, 2004; Tomlinson *et al.*, 2004). Patients with metabolic syndrome are therefore at increased risk of coronary heart disease, stroke and type 2 diabetes. Cushing's syndrome, which has many symptoms resembling metabolic syndrome, is also correlated with excess cortisol (Asensio *et al.*, 2004; Mariniello *et al.*, 2006). Inhibiting 11β-HSD1 is therefore seen as a promising treatment for metabolic syndrome and other metabolic diseases. This hypothesis has been further strengthened by studies in animal models (Masuzaki *et al.*, 2001; Morton *et al.*, 2001, 2004; Kotelevtsev *et al.*, 1997; Alberts *et al.*, 2002, 2003).

Although several different classes of potent and selective inhibitors of 11β-HSD1 have been reported to date, with many the result of efforts in structure-based drug design (Hale *et al.*, 2008; Johansson *et al.*, 2008; Julian *et al.*, 2008; Sun *et al.*, 2008; Tu *et al.*, 2008; Wan *et al.*, 2009), in our research efforts we were unable to generate complex structures of 11β-HSD1 with our specific synthesized ligands using commonly utilized complexation methods. In each case the detergent

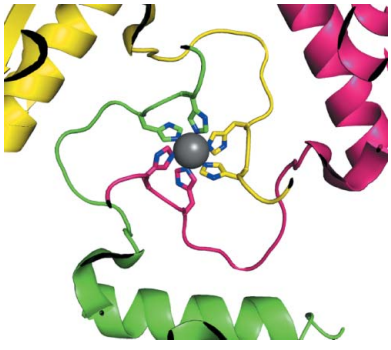

which was necessary for protein solubilization also occupied the active site and was not displaced by our compounds. In order to obtain the required complexes with our specific ligands, we therefore developed an on-column ligand- and detergent-exchange method prior to crystallization which allowed us to generate protein–ligand crystal structures. In this study, we report the on-column exchange method and an unexpected assembly of the protein N-terminal tags in the crystal packing.

2. Materials and methods

The methods for cloning, expression and initial purification for crystallization trials of 11β-HSD1 followed the method described by Hosfield *et al.* (2005) with some adaptation. These are briefly described as follows.

2.1. Cloning and expression

A recombinant N-terminally truncated form of human 11β-HSD1 with a C-terminal domain cysteine point mutation {6(HQ)-[11β-HSD-1 (24–292) C272S]} was expressed in *Escherichia coli* DH10b-Tir cells. The cells were plated on Luria broth–ampicillin (200 mg l^{-1}) plates overnight. The next day, fresh transformants were used to inoculate Fernbach flasks containing 1 l Luria broth and carbenicillin (200 mg l^{-1}). Cells were grown at 310 K to an OD of 0.41; the cultures were then supplemented with 0.25 m*M* corticosterone, the flasks were shifted to 303 K and expression was induced by the addition of 0.2% arabinose. The cells were harvested 5 h post-induction by centrifugation and frozen at 188 K.

2.2. Purification of 11β-HSD1 for initial crystallization experiments

Frozen cells were resuspended in lysis buffer (50 m*M* Tris, 150 m*M* NaCl, 30 m*M* CHAPS {3-[(3-cholamidopropyl)dimethylammonio]-1-propanesulfonate} pH 7.9, 40 µg ml^{-1} Benzonase, 2 µl ml^{-1} Ready-Lyse (Epicentre Biotechnologies, Madison, Wisconsin, USA)), lysed, incubated at room temperature for 1 h and clarified by centrifugation at 28 000*g* for 30 min to remove insoluble material. The supernatant was then passed through a 0.45 µm vacuum filter and loaded onto an Ni–IDA ProBond column (Invitrogen, Carlsbad, California, USA). The column was washed with loading buffer (50 m*M* Tris pH 7.6, 4 m*M* CHAPS, 40 m*M* imidazole, 250 m*M* NaCl) and eluted isocratically with elution buffer (loading buffer with 200 m*M* imidazole pH 7.8). This was followed by a Sephadex G-25 column (GE Healthcare, Piscataway, New Jersey, USA) with running buffer consisting of 25 m*M* Tris, 250 m*M* NaCl, 4 m*M* CHAPS pH 7.6. Fractions identified as 11β-HSD1 by SDS–PAGE were pooled and concentrated to 11 mg ml^{-1} using a 10 kDa membrane cutoff Amicon Centriprep (Millipore, Billerica, Massachusetts) at 277 K.

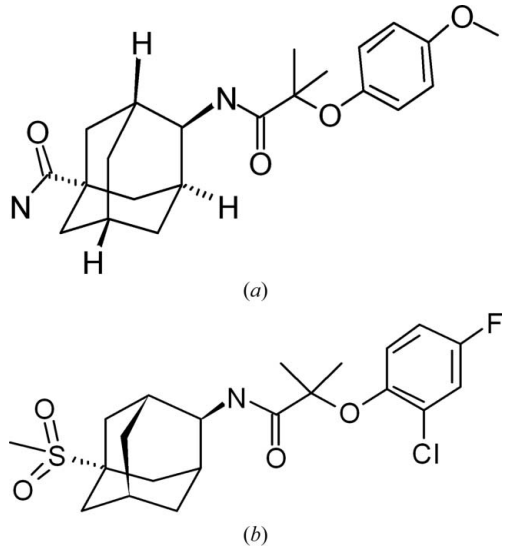

Figure 1
Representative compounds reported in this study: (*a*) (1*S*,3*S*,4*S*,5*R*,7*S*)-4-[2-(4-methoxyphenoxy)-2-methylpropionylamino]-adamantane-1-carboxylic acid amide (compound 1), (*b*) 2-(2-chloro-4-fluorophenoxy)-*N*-[(1*R*,2*S*,5*S*,7*S*)-5-methanesulfonyl-adamantan-2-yl]-2-methylpropionamide (compound 2).

2.3. Adamantane-class compounds

The compounds for which complex structures were pursued in this study were adamantane-class compounds. Two compounds from this class, (1*S*,3*S*,4*S*,5*R*,7*S*)-4-[2-(4-methoxyphenoxy)-2-methylpropionylamino]-adamantane-1-carboxylic acid amide (listed as compound 1) and 2-(2-chloro-4-fluorophenoxy)-*N*-[(1*R*,2*S*,5*S*,7*S*)-5-methanesulfonyl-adamantan-2-yl]-2-methylpropionamide (listed as compound 2), were used as representative compounds in this report. Their molecular structures are illustrated in Fig. 1. The compounds were synthesized as reported previously (Patel *et al.*, 2007; Sorensen *et al.*, 2007).

2.4. Purification with on-column 11β-HSD1–ligand complexation

After cell lysis (as described above), the supernatant was divided into 100 ml volumes and purified in parallel. Each 100 ml volume was loaded onto 5 ml Probond resin (Invitrogen, Carlsbad, California, USA) previously equilibrated with three column volumes of wash buffer (50 m*M* Tris, 300 m*M* NaCl, 40 m*M* imidazole, 4 m*M* CHAPS pH 7.9). The resin was washed with 20 column volumes of wash buffer, gradiented to 100% overnight buffer {50 m*M* Tris, 300 m*M* NaCl, 5%(*v*/*v*) glycerol, 0.05%(*v*/*v*) Triton X-100, 0.5 m*M* $MgCl_2$, 2 m*M* ATP, 2 m*M* TCEP [Tris(2-carboxyethyl)phosphine], 20 µ*M* inhibitor pH 7.9} in ten column volumes and then isocratically run with another 20 column volumes of overnight buffer. Next morning, each column was washed with buffer *A* [50 m*M* Tris, 300 m*M* NaCl, 5%(*v*/*v*) glycerol, 0.05%(*v*/*v*) Triton X-100, 2 m*M* TCEP, 2.5 µ*M* inhibitor pH 7.9] for ten column volumes followed by 2% buffer *B* (2 *M* imidazole pH 7.8) for eight column volumes, 3% buffer *B* for three column volumes, 10% buffer *B* for eight column volumes and finally 15% buffer *B* for three column volumes. The fractions containing 11β-HSD1 as assayed by SDS–PAGE were pooled and run on a Sephadex G-25 (GE Healthcare, Piscataway, New Jersey) column with running buffer consisting of 20 m*M* Tris, 250 m*M* NaCl, 5%(*v*/*v*) glycerol, 2 m*M* TCEP, 0.05%(*v*/*v*) Triton X-100, 2 µ*M* inhibitor pH 8.0 and then concentrated to 12–15 mg ml^{-1}. Part of the protein was immediately used for crystallization screening. The rest of the protein was flash-frozen in 60 µl aliquots for further crystallization optimization experiments if needed. Initially, the on-column experiments were conducted at 277 K with no NaCl in the size-exclusion column buffer. Subsequent on-column exchange experiments were conducted at room temperature with 250 m*M* NaCl added to the size-exclusion buffer to promote protein stability during the concentration step.

2.5. Crystallization

All crystallization experiments were conducted by vapor diffusion at 277 K. Samples were initially screened and promising hits were then further optimized using drops consisting of 2 µl protein solution

and 2 µl reservoir solution equilibrated against 1 ml reservoir solution. For the complex with compound 1 (15 mg ml^{-1}), the reservoir solution was 2.0 *M* ammonium sulfate, 0.1 *M* trisodium citrate dihydrate pH 5.6, 0.2 *M* potassium/sodium tartrate tetrahydrate. In this instance the protein buffer did not contain 250 m*M* NaCl, which was added to all subsequent samples to improve protein stability during concentration. For the complex with compound 2 (13 mg ml^{-1}), the reservoir solution was 2.2 *M* ammonium sulfate, 0.1 *M* trisodium citrate dihydrate. In both cases the crystals were cryoprotected using 26%(*v*/*v*) glycerol and X-ray diffraction data were collected on the 17-BM beamline at the Advanced Photon Source.

2.6. Structure determination

Diffraction data were indexed, integrated and scaled using *HKL*-2000 (Otwinowski & Minor, 1997) and the structures were solved by molecular replacement with *MOLREP* (Vagin & Teplyakov, 2010) in the *CCP*4 program suite (Winn *et al.*, 2011) using PDB entry 1xu9 (Hosfield *et al.*, 2005) as a model. The models were refined iteratively using the graphics programs *QUANTA* (Accelrys, San Diego, California, USA) and *REFMAC*5 (Murshudov *et al.*, 2011). Figures were prepared using the program *PyMOL* (Schrodinger LLC).

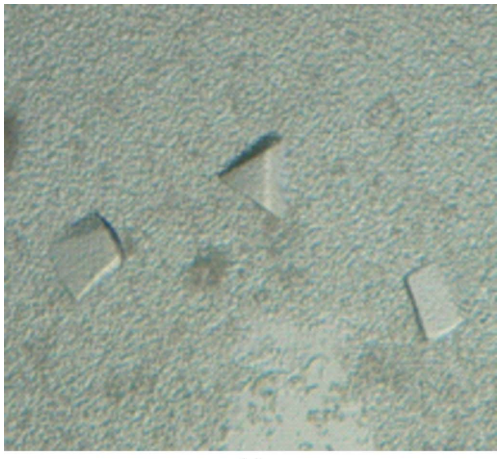

(*a*)

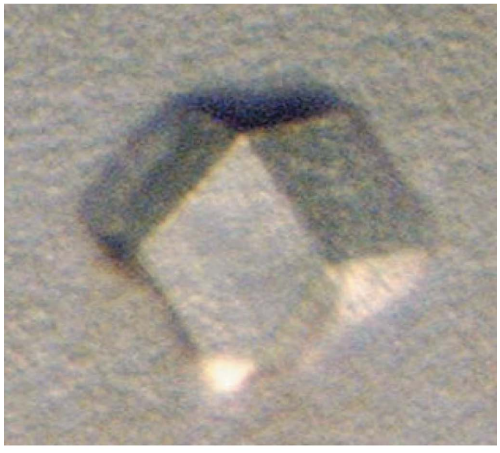

(*b*)

Figure 2
Crystal morphologies obtained during the course of the 11β-HSD1 complex crystallization experiments: (*a*) trigonal (compound 1), (*b*) cubic (compound 2).

3. Results

3.1. Initial 11β-HSD1–ligand complex structure attempts

An initial crystal structure of 11β-HSD1 prepared in the absence of ligands reproduced the findings of Hosfield *et al.* (2005) in that CHAPS was observed in the active site (data not shown). Attempts to soak these crystals with specific ligands of interest were unsuccessful. The crystals either did not survive the soaking process or provided poor diffraction. To stabilize the crystals during soaking the crystals were cross-linked with glutaraldehyde (Lusty, 1999). These crystals looked good visually after soaking, but still did not provide usable diffraction. Attempts were then made to obtain complex structures by cocrystallization. Adding ligand in excess to the protein (by straight addition or *via* dialysis) and incubating prior to setting up crystallization plates provided crystals with useful diffraction; however, it was observed that CHAPS was still not displaced from the active site. Diluting the protein and ligand in order to make a low-concentration complex with a reduced CHAPS concentration (1 m*M*) in the buffer and then concentrating back to a usable protein concentration prior to crystallization gave the same unsuccessful result. An attempt was also made to include the ligand in the ferment and have it present throughout the purification process; however, this also proved to be unsuccessful.

3.2. On-column complexation of 11β-HSD1 with inhibitors

To obtain a successful complex it appeared to be important to keep the protein stable in the presence of CHAPS (which serves as both a solubilizing agent and a stabilizing ligand) in the first step of the preparation. It was then necessary to find a method that allowed CHAPS to be exchanged with another solubilizing detergent that had no affinity for the active site while forming the desired ligand complex. The method developed for this purpose was to immobilize the protein on a Probond resin column and then exchange CHAPS with Triton X-100 while the ligand was present in the buffer. This provided the necessary exchange while also stabilizing the protein and preventing protein aggregation during exchange. A typical final

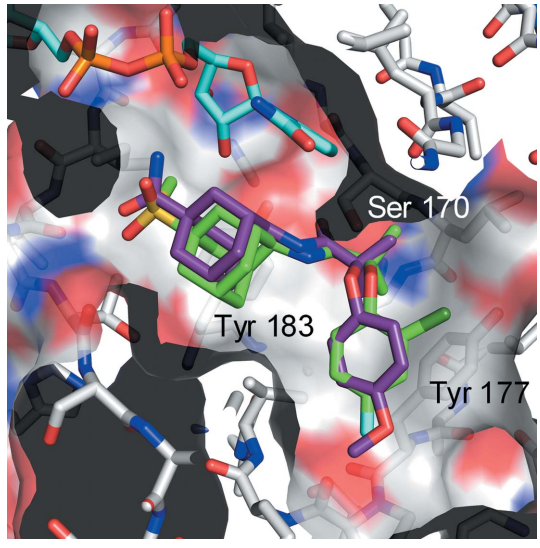

Figure 3
Overlay of the crystal structures of 11β-HSD1 with compound 1 (purple) and compound 2 (green). The protein is colored gray and the NADP$^+$ cofactor is highlighted in cyan. Elemental components are colored as follows: oxygen, red; nitrogen, blue; sulfur, yellow; phosphate, orange; chlorine, dark green; fluorine, light blue.

Table 1
X-ray diffraction and refinement statistics.

Values in parentheses are for the highest resolution shell.

PDB code	2irw	2ilt
X-ray diffraction		
Beamline	APS 17-ID	APS 17-BM
Wavelength (Å)	1.000	1.000
Space group	*H*32	*I*23
Unit-cell parameters (Å, °)	$a = b = 184$, $c = 558$, $\alpha = \beta = 90$, $\gamma = 120$	$a = b = c = 124$, $\alpha = \beta = \gamma = 90$
Resolution (Å)	3.1 (3.21–3.10)	2.3 (2.38–2.30)
Observations	371110	150002
Unique observations	66694 (6590)	14223 (1413)
Completeness (%)	99.9 (100)	99.9 (100)
$\langle I/\sigma(I)\rangle$	7.2 (4.2)	13.7 (4.7)
$R_{\rm merge}$† (%)	11.3 (48)	6.7 (47)
Model refinement		
Reflections (working/free)	63307/3377	12794/713
Completeness (working/free) (%)	95/5	95/5
$R_{\rm work}/R_{\rm free}$‡ (%)	23.7/27.8	20.9/27.5
Mean *B* factor (Å^2)	42	36
R.m.s.d. ideal bond lengths (Å)	0.014	0.010
R.m.s.d. ideal bond angles (°)	1.25	1.31

† $R_{\rm merge} = \sum_{hkl}\sum_i |I_i(hkl) - \langle I(hkl)\rangle| / \sum_{hkl}\sum_i I_i(hkl)$, where $I(hkl)$ is the integrated intensity of a reflection. ‡ $R_{\rm work} = \sum_{hkl} ||F_{\rm obs}| - |F_{\rm calc}|| / \sum_{hkl} |F_{\rm obs}|$, where $F_{\rm obs}$ and $F_{\rm calc}$ are the observed and calculated structure-factor amplitudes; $R_{\rm free}$ is calculated using 5% of the data that were excluded from refinement.

yield for each protein–inhibitor preparation was 1.5 mg per gram of cells.

Of 11 unique complexes generated using this protocol, six provided crystals, giving a 55% success rate for crystallization. While all of the complexes were broadly screened, the useable crystallization hits tended to be clustered around ammonium sulfate conditions (1.6–3.0 *M*) within the pH range 5.6–8.5. Of the six crystallization leads, one could not be optimized to provide usable crystals and one did not provide diffraction data of sufficiently high quality to distinguish the ligand. A total of four structures were obtained (with diffraction resolutions of 2.3, 2.4, 2.5 and 3.1 Å) from the 11 on-column ligand-exchange experiments, providing a structure-to-experiment success rate of 36%. For those crystals providing structures, two different crystal morphologies were obtained. Compound 1 produced trigonal crystals, while the other three compounds, including compound 2, produced cubic crystals (Fig. 2).

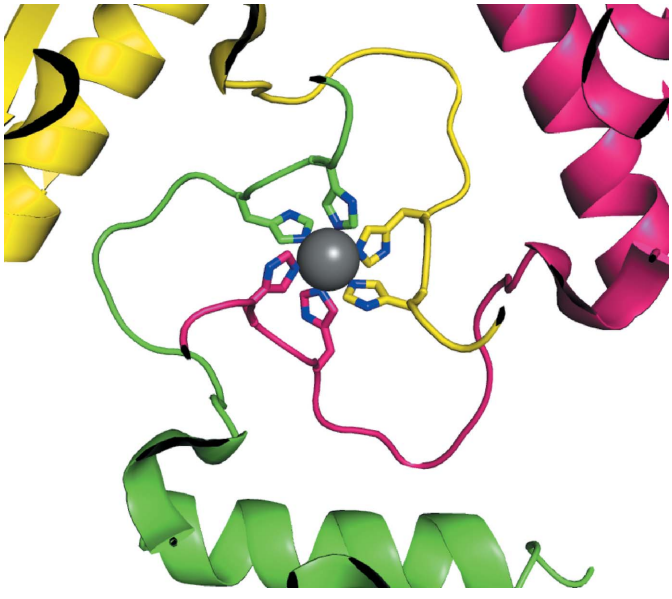

Figure 4
Chelation of metal ions by the 6(HQ) N-terminal purification tag, forming an artificial trimer in the crystal. Only the histidine residues of the tag coordinating the ion are illustrated. Each 11β-HSD1 monomer is represented in a different color.

3.3. Representative crystal complex structures

Fig. 3 shows an overlay of the structures of 11β-HSD1 complexed with compound 1 (PDB entry 2irw; Patel *et al.*, 2007) and compound 2 (PDB entry 2ilt; Sorensen *et al.*, 2007). Both compounds displayed a similar binding mode in the steroid-binding site adjacent to the bound cofactor NADP$^+$, with the adamantyl moiety of each compound located near the nicotinamide portion of the cofactor. For compound 1 the primary amide is positioned close to the pyrophosphates of the NADP$^+$. The central amide interacts with the active-site residues; the carbonyl is within 2.8 and 2.9 Å of the hydroxyl groups of Ser170 and Tyr183, respectively. The *gem*-dimethyl and ether-linked phenyl groups extend into the hydrophobic cavity of the steroid-binding site, where Tyr177 forms the base of the pocket. The binding of compound 2 is similar, with the central carbonyl interacting with the same key residues responsible for substrate ketone reduction. X-ray diffraction statistics for both structures are given in Table 1.

3.4. Metal-ion chelation by the purification tag in the crystal structures

Upon further inspection of the crystal structures, an unexpected chelation of metal ions by the purification tag was observed in three of the four structures. In the structure with compound 1, in which the crystals grew in a trigonal crystal form, the N-terminal purification tag 6(HQ) was disordered. However, in the other three structures, in which the crystals grew in a cubic form, it was observed that the tag was chelating metal ions (possibly nickel ions stripped from the column as a result of the on-column exchange), forming an artificial trimer (Fig. 4). The chelation of the metal is facilitated by the tag, as the histidine residues chelate the metal ions while the alternating glutamine residues flip out and away from the ions.

4. Discussion

The first structure of human 11β-HSD1 was published by Hosfield *et al.* (2005). In this structure, the cofactor NADP$^+$ and the steroidal detergent CHAPS that was used in the purification were identified in the active site. Since then, researchers pursuing ligand-complex structures with human 11β-HSD1 have also noted CHAPS in the binding site, but were able to displace the CHAPS by soaking (Hale *et al.*, 2008; Tu *et al.*, 2008; Wan *et al.*, 2009) or by cocrystallization (Johansson *et al.*, 2008; Julian *et al.*, 2008; Sun *et al.*, 2008) with their ligands of interest. Although we used a similar cloning and purification procedure, we were unable to displace CHAPS with our adamantane compounds by soaking, cocrystallization or other commonly used complexation procedures. While this is puzzling, another researcher working with guinea pig 11β-HSD1 also reported problems in ligand exchange (Ogg *et al.*, 2005). In this case, the protein was incubated during purification with NADP$^+$ and ligand (BVT.4584). An attempt was then made to exchange this set of ligands with AADP and cortisone by repeated dilution and re-concentration of the protein in the presence of the new cofactor and ligand prior to crystallization. When the structure was solved, NADP$^+$ was found to be present; however, neither cortisone nor BVT.4584 was observed in the binding site, indicating that the ligand-exchange exercise had not been successful. Although we made multiple attempts to obtain complex structures with our adamantane compounds by a variety of methods, only by using the on-column

exchange method were we able to obtain the desired complex structures.

The ligand–protein complexes produced by the on-column method had a crystallization success rate of 55%. This is typical in our experience of that encountered in cocrystallization experiments. For example, the success rate of ligand cocrystallization with Hsp90 (heat-shock protein 90; Huth *et al.*, 2007) in our laboratory was 50%. For 11β-HSD1, despite broad screening, a clustering of crystallization conditions was observed, but this again is typical in our experience of that encountered when cocrystallizing with compounds from within the same chemical series.

One unexpected result from the on-column exchange experiments was the observed chelation of metal ions by the 6(HQ) N-terminal tag, which resulted in an artificial trimer in the crystal structures. In our initial structure with $NADP^+$ and CHAPS, as also in the reported literature structure using the same clone (Hosfield *et al.*, 2005), the N-terminus was disordered. For the first compound used in the on-column exchange experiments (compound 1) the resulting crystals were in a trigonal form and the N-terminus was also disordered in the structure. However, the next three structures, for which compound 2 is representative, all grew in a cubic crystal form and all showed the artificial trimer (with the chelated metal ions) in the structure.

There are a number of possible factors for this variance in the crystallization results from the on-column exchange experiments. In the first attempt with compound 1 the on-column exchange was conducted at 277 K, while all subsequent experiments were conducted at 296 K. Also, for compound 1 the protein buffer during the final concentration step did not contain the 250 m*M* NaCl that was added to all subsequent samples to improve the protein stability during concentration. The ligands can also affect crystallization. Compound 1 has an amide terminal to the adamantane, yet similar compounds were also present among the complexes that formed the artificial trimers. The most likely factor is therefore the crystallization conditions, to which the differing NaCl concentration in the protein buffer may have contributed. For compound 1 the crystals grew at pH 5.6. For the three complexes that formed the artificial trimers, the crystallization solution pH was 7.1–7.3. This higher pH range is more favorable for the chelation of metal ions with a histidine-based tag than pH 5.6. For the complexes that provided the artificial trimers, dynamic light scattering of diluted samples (18 μM) revealed that 98–99% of the mass had a size of 5 nm, indicative of monomers. The trimer is therefore likely to form at higher protein concentrations under crystallization conditions where the pH is more favorable for metal-ion chelation. At this point the metal ions are assumed to be nickel that was stripped from the column during the process of on-column exchange; however, this has not been confirmed.

5. Conclusions

For the adamantane compounds pursued in this study, the on-column exchange method provided 11β-HSD1–ligand complexes for structure determination where other reported complexation methods had not been successful. The crystallization success rates for the on-column exchange method are similar to those achieved by traditional cocrystallization methods. One interesting byproduct of the method was the chelation of metal ions by the 6(HQ) tag, which produced artificial trimers in the crystal structures. The on-column exchange method should be considered for the production of protein–ligand complexes in cases where traditional complexation methods are not successful.

We thank J. R. Patel and B. Sorensen for providing the adamantane compounds listed in this study, D. Bartley for the fermentation of the protein constructs and U. S. Ladror for providing expertise and assistance with the parallel purification of protein samples. X-ray diffraction data were collected on beamline 17-BM in the facilities of the Industrial Macromolecular Crystallography Association Collaborative Access Team (IMCA-CAT) at the Advanced Photon Source. These facilities are supported by the companies of the Industrial Macromolecular Crystallography Association.

References

Alberts, P., Engblom, L., Edling, N., Forsgren, M., Klingström, G., Larsson, C., Rönquist-Nii, C., Ohman, B. & Abrahmsén, L. (2002). *Diabetologia*, **45**, 1528–1532.
Alberts, P. *et al.* (2003). *Endocrinology*, **144**, 4755–4762.
Asensio, C., Muzzin, P. & Rohner-Jeanrenaud, F. (2004). *Int. J. Obes.* **28**, S45–S52.
Hale, C., Véniant, M., Wang, Z., Chen, M., McCormick, J., Cupples, R., Hickman, D., Min, X., Sudom, A., Xu, H., Matsumoto, G., Fotsch, C., St Jean, D. J. & Wang, M. (2008). *Chem. Biol. Drug Des.* **71**, 36–44.
Hassell, A. M. *et al.* (2007). *Acta Cryst.* D**63**, 72–79.
Hosfield, D. J., Wu, Y., Skene, R. J., Hilgers, M., Jennings, A., Snell, G. P. & Aertgeerts, K. (2005). *J. Biol. Chem.* **280**, 4639–4648.
Huth, J. R. *et al.* (2007). *Chem. Biol. Drug Des.* **70**, 1–12.
Johansson, L. *et al.* (2008). *J. Med. Chem.* **51**, 2933–2943.
Julian, L. D. *et al.* (2008). *J. Med. Chem.* **51**, 3953–3960.
Kotelevtsev, Y., Holmes, M. C., Burchell, A., Houston, P. M., Schmoll, D., Jamieson, P., Best, R., Brown, R., Edwards, C. R. W., Seckl, J. R. & Mullins, J. J. (1997). *Proc. Natl Acad. Sci. USA*, **94**, 14924–14929.
Lusty, C. J. (1999). *J. Appl. Cryst.* **32**, 106–112.
Mariniello, B., Ronconi, V., Rilli, S., Bernante, P., Boscaro, M., Mantero, F. & Giacchetti, G. (2006). *Eur. J. Endocrinol.* **155**, 435–441.
Masuzaki, H., Paterson, J., Shinyama, H., Morton, N. M., Mullins, J. J., Seckl, J. R. & Flier, J. S. (2001). *Science*, **294**, 2166–2170.
Morton, N. M., Holmes, M. C., Fiévet, C., Staels, B., Tailleux, A., Mullins, J. J. & Seckl, J. R. (2001). *J. Biol. Chem.* **276**, 41293–41300.
Morton, N. M., Paterson, J. M., Masuzaki, H., Holmes, M. C., Staels, B., Fievet, C., Walker, B. R., Flier, J. S., Mullins, J. J. & Seckl, J. R. (2004). *Diabetes*, **53**, 931–938.
Murshudov, G. N., Skubák, P., Lebedev, A. A., Pannu, N. S., Steiner, R. A., Nicholls, R. A., Winn, M. D., Long, F. & Vagin, A. A. (2011). *Acta Cryst.* D**67**, 355–367.
Ogg, D., Elleby, B., Norström, C., Stefansson, K., Abrahmsén, L., Oppermann, U. & Svensson, S. (2005). *J. Biol. Chem.* **280**, 3789–3794.
Otwinowski, Z. & Minor, W. (1997). *Methods Enzymol.* **276**, 307–326.
Patel, J. R. *et al.* (2007). *Bioorg. Med. Chem. Lett.* **17**, 750–755.
Rosmond, R. (2004). *Psychoneuroendocrinology*, **30**, 1–10.
Sorensen, B. *et al.* (2007). *Bioorg. Med. Chem. Lett.* **17**, 527–532.
Sun, D. *et al.* (2008). *Bioorg. Med. Chem. Lett.* **18**, 3513–3516.
Tomlinson, J. W., Walker, E. A., Bujalska, I. J., Draper, N., Lavery, G. G., Cooper, M. S., Hewison, M. & Stewart, P. M. (2004). *Endocr. Rev.* **25**, 831–866.
Tu, H. *et al.* (2008). *Bioorg. Med. Chem.* **16**, 8922–8931.
Vagin, A. & Teplyakov, A. (2010). *Acta Cryst.* D**66**, 22–25.
Wan, Z.-K. *et al.* (2009). *J. Med. Chem.* **52**, 5449–5461.
Winn, M. D. *et al.* (2011). *Acta Cryst.* D**67**, 235–242.